Techno-economic optimization of open-air swimming pool heating system with PCM storage tank for winter applications

Yantong Li[a,b], Zhixiong Ding[c], Yaxing Du[d,*]

[a]Department of Architecture and Civil Engineering, City University of Hong Kong, Tat Chee Avenue, Kowloon, Hong Kong, China

[b]Department of Energy and Process Technology, Norwegian University of Science and Technology, Kolbjørn Hejes vei 1 B, Trondheim, Norway

[c]School of Energy and Environment, City University of Hong Kong, Tat Chee Avenue, Kowloon, Hong Kong, China

[d]Department of Particulate Flow Modelling, Johannes Kepler University, Linz, Austria

***The corresponding author; Tele: +43 732 2468 6489; +43 732 2468 6462; Email: yaxing.du@gmail.com

ABSTRACT

Feasible heating systems have been designed to increase the availability of open-air swimming pools in winter in subtropical climate regions. However, the approach to optimally size the main components of the system from multiple aspects is lacking. A techno-economic optimization method for swimming pool heating systems is proposed here. Minimizing the lifecycle cost of the system while ensuring the thermal comfort of the pool are considered as the optimization objectives. The volume of phase change material storage tank and the heating capacity of air-source heat pumps are selected as design variables. To improve computational efficiency, surrogate models are developed using the response surface approach, in which the dataset is generated from the simulation platform established using MATLAB and TRNSYS. Generic algorithm and non-dominated sorting genetic algorithm II are adopted to conduct single-objective and double-objective optimizations, respectively. Case studies indicate that optimal combinations for the size of main components can be identified using the proposed optimization approach. The energy and economic performance of the heating system are enhanced after optimization. The proposed techno-economic optimization method

provides an instructive guideline for the optimal design of swimming pool heating systems.

Keywords: Phase change material; Techno-economic optimization; Open-air swimming pool; Heating system

1 Nomenclature

Abbreviations		q_{amc}	required heating capacity of ASHPs for charging purpose
ASHP	air-source heat pump	q_{amp}	required heating capacity of ASHPs for preheating purpose
CCD	Central Composite Design	q_{an}	minimum design value of q_{ashp}
COP	coefficient of performance	q_{ashp}	capacity of ASHPs
DOE	Design of Experiments	q_{lt}	heat loss from cover
GA	generic algorithm	q_{pa}	heat obtained from PST or ASHPs
NSGA-II	non-dominated sorting genetic algorithm II	q_t	total heat transfer rate of pool
PCM	phase change material	r	electricity increasing rate
POS	Pareto optimal solution	sp_p	simple payback period
PST	PCM storage tank	TP	time percentage of thermal comfort unmet
PV	photovoltaic	T_c	cover temperature
RSA	response surface approach	T_{dp}	design pool water temperature
TEO	techno-economic optimization	T_{dt}	design temperature that the PST should be heated up to during the charging process
		T_m	PCM melting temperature
		T_p	pool water temperature
Symbols		T_{pai}	inlet water temperature of heat exchanger on load side
A_t	cover area	T_{pao}	outlet water temperature of heat exchanger on load side
a	market discount rate	T_{pm}	PCM temperature
a_k	first-order factor	T_w	water temperature
a_{kk}	second-order factor	t	time
a_{kj}	interaction effect coefficient	t_o	total opening time of swimming pool during the entire winter season
a_0	intercept value	tc_u	indicator to evaluate thermal comfort

			requirement of the pool
c_l	specific heat of liquid PCM	te_o	required maximum thermal energy during the open period
c_s	specific heat of solid PCM	te_p	required maximum thermal energy during the preheating period
c_w	specific heat of water	V_p	pool volume
e_d	energy use of developed system	V_{pm}	maximum design value of V_{pst}
e_{sr}	energy saving ratio	V_{pst}	volume of PST
e_t	energy use of traditional system	V_{pn}	minimum design value of V_{pst}
ee	random error	v_w	mean velocity of water
f_{pm}	melting or solidification fraction of PCM	W	response parameter
H_{pm}	enthalpy of PCM	x	distance
h_t	volumetric heat transfer coefficient between water and PCM	Y_j	j^{th} decision variable
h_{tp}	heat transfer coefficient between cover and pool	Y_k	k^{th} decision variable
ic	initial cost		
ic_a	initial cost of ASHPs		
ic_{ds}	initial investment of developed system	*Greek symbols*	
ic_o	initial cost of other components	ε_w	water fraction
ic_p	initial cost of PST	ρ_w	water density
k_w	thermal conductivity of water	ρ_{pm}	PCM density
LC	system lifecycle cost	φ_n	user-defined factor for minimum design values
m_w	water flowrate	ΔH_m	latent heat of PCM
oc	operating cost	Δ_s	user-defined threshold for thermal comfort of the pool water temperature
oc_{ds}	operating cost of developed system	Δt	time span

oc_{sr}	operating cost saving ratio	Δt_c	time span of charging process
oc_{ts}	operating cost of traditional system	Δt_p	time span of preheating process
oc_1	operating cost in first year within project lifetime	Δx	distance span
q_{am}	maximum design value of q_{ashp}		

1. Introduction

Most open-air swimming pools in subtropical regions are closed in winter because the energy demand required for satisfying the thermal comfort of the pool is high. If conventional heating approaches such as electrical heaters are adopted to supply heat to pools, the expense will be extremely high [1]. Therefore, various techniques have been used to increase the availability of pools in winter. These techniques can be divided into two roles: passive and active approaches. The passive approach primarily uses a thermal-insulation cover to prevent heat losses when the pool is closed. Different studies regarding the passive approach have been conducted. For example, Yadav et al. [2] modeled the water temperature variation of an Australian swimming pool with thermal-insulation cover. They concluded that the heat losses of the pool could be significantly reduced when the cover was used. In the study by Francey et al. [3], thermal insulation properties with transparent and opaque covers used in pools were compared by analyzing the in-situ measured water temperature of the pool. They discovered that the transparent cover was more effective in improving the water temperature than the opaque cover because more solar energy could be obtained by the pool water when the transparent cover was used.

The active approach is developed to provide heat for satisfying the heat demand of pools. One typically used method is air-source heat pumps (ASHPs). Lam et al. [4, 5] used ASHPs to supply heat to a swimming pool in a hotel in Hong Kong. The surface area and volume of the pool were 35 m^2 and 52 m^3, respectively. The energy saving analysis of the system was performed, and the lifecycle energy cost of the system was calculated. They concluded that, compared with traditional heating technologies, the energy cost with a lifecycle period of 10 years could be reduced by HK$275,700 if ASHPs with a coefficient of performance (COP) of 3.5 was installed. However, the designed heating capacity of the ASHPs should be identified by the peak heating load of the pool. For pools with a large peak heating load (e.g., pools with large surface area), the designed heat capacity of the ASHPs should be large, which results in a high capital cost for installing ASHPs. To tackle with this problem, Li et al. [6] proposed a heating system with PST (i.e., storage tank with phase change material (PCM)) to completely shift the energy use from on-peak to off-peak periods, which could reduce the operating cost significantly. The ASHPs were not used to supply heat to the pool during the on-peak period but to charge the PST during the off-peak period. Therefore, the designed heat capacity of the ASHPs was not based on the peak heat load of the pool, and it could be reduced.

The approach that adopts the PST to shift the electricity use from on-peak to off-peak periods has been extensively investigated for building energy systems. For instance, Comodi et al. [7] conducted the economic analysis of a cold energy storage system with a PST in different tariff scenarios, and the economic benefits was estimated. They discovered that a shorter payback period of the system could be obtained if the electricity tariff difference between the on-peak and off-peak periods was larger. Burno et al. [8] utilized a PST in a chiller cooling system, and they reported that 85% of the energy consumed by the system could be shifted from the on-peak to off-peak periods when a PST was used. In addition, a 13.5% energy reduction could be obtained when the PCM had a melting temperature of 10 °C. Najafian et al. [9] conducted the optimal design of a domestic hot water system with PST and determined the minimum amount of PCM by the generic algorithm (GA). It was concluded that the energy consumed during the on-peak period could be completely shifted to the off-peak period with the optimal amount of PCM. Nkwetta et al. [10] investigated the performance of a residential hot water system with PST and discovered that the energy performance of the system could be improved using the proposed control strategy. However, the approach where the PST is used to shift the electricity consumed from on-peak to off-peak periods is rarely applied in swimming pool heating systems. It should be mentioned that even though the PST was used in the study of Zsembinszki et al. [11] to provide heat for the pool, the approach has not been adopted.

From the abovementioned swimming pool heating techniques, it can be concluded that a thermal-insulation cover is efficient for preventing heat loss when a pool is closed; additionally, ASHPs integrated with a PST can effectively enhance the economic performance of the system. Hence, it will be meaningful to develop a swimming pool heating system that comprehensively utilizes these techniques for a better performing system. However, it is challenging to optimize the size of the main components in complex heating systems to satisfy multiple objectives (e.g., reliability and economic performance).

The techno-economic optimization (TEO) can effectively improve the reliability and economic performance of the system [12, 13]. Kaabeche and Ibtiouen [14] performed TEO for an energy system comprising photovoltaic (PV) panels, wind turbines, diesel, and batteries. Amrollahi and Bathaee [15] performed the TEO of a stand-alone grid system with PV panels, wind turbines, and batteries, considering the effect of a demand response program. It was discovered that the capacity of PV panels and the number of batteries could be reduced when the demand response program was adopted. Jamshidi and Askarzadeh [16] conducted the TEO of a power generation system comprising PV panels, diesel generators, and fuel cells. They reported that the total expense of the system could be reduced when the hydrogen energy technique was adopted. Although TEO methods for various building energy systems have been proposed, the approach for conducting the TEO of the swimming pool heating system is still lacking.

Therefore, a TEO method for swimming pool heating systems is proposed here. The optimization objective is to minimize the system's lifecycle cost while ensuring the desired thermal comfort of the pool. The volume of the PST and the heat capacity of the ASHPs were selected as the design variables. To enhance computational efficiency, the response surface approach (RSA) was adopted to develop the surrogate models. The simulation platform of the system was constructed using TRNSYS and MATLAB. The GA and non-dominated sorting genetic algorithm II (NSGA-II) were utilized to perform single-objective and double-objective optimizations, respectively. The control, energy, and economic performance of the system with the optimal system configuration are analyzed.

The novelty of this study is presented as follows: (1) The proposed TEO method fills the knowledge gap pertaining to the optimal design of open-air swimming pool heating systems, which considers lifecycle cost as the economic indicator and the desired thermal comfort of the pool as the reliability indicator; (2) The surrogated model of the complex heating system, which is developed using the RSA, can effectively enhance computational efficiency and is highly reliable. Its application can be extended to other building heating or cooling systems; (3) Single-objective and double-objective optimizations of the system are performed using optimization algorithms, i.e., GA and NSGA-II, respectively, and the optimal design solutions can be effectively identified; (4) The case study of an advanced heating system for open-air swimming pools in winter in subtropical climates is conducted to demonstrate the applicability and efficiency of the proposed TEO method.

2. Methodology

2.1. Methodology for techno-economic optimization

The framework for the methodology of the TEO is depicted in Fig. 1. This methodology comprises three primary steps: development of surrogate models for objective functions, TEO, and performance analysis. In the first step, professional software (e.g., DESIGN EXPERTS) can be used to design a set of simulated experiments. Based on predefined upper and lower bound values of the design variables, the design dataset will be determined. The generated dataset of the design variables will be used as the input for the complex simulation platform, and the corresponding values of the objective functions in the TEO can be obtained. The complex simulation platform typically comprises heat transfer models, control strategies, meteorological data, and operating parameters. Surrogate models will be developed by statistical methods (e.g., RSA). In the second step, the TEO of the system will be performed using the optimization algorithms (i.e., GA and NASG-II), and the optimal solutions will be obtained. In the final step, the system performance with the optimal system configurations will be analyzed using different performance indices.

2.2. Optimization objectives and design variables

The volume of the PST (V_{pst}) and the heating capacity of the ASHPs (q_{ashp}) were selected as design variables. Two optimization objectives were considered: minimizing the thermal comfort unmet time percentage (TP) and minimizing the lifecycle cost of the system (LC). TP was used to assess the reliability of the system, which is defined by the total time that thermal comfort is unsatisfied divided by the total open time of the pool during the entire winter. It is expressed as the following equation:

$$TP = \frac{1}{t_o}\int_0^{t_o} tc_u dt \quad (1)$$

where t_o is the total time that the pool is open during the entire winter season; tc_u is an indicator to evaluate the thermal comfort of the pool, which is expressed as the following equation:

$$tc_u = \begin{cases} 0 & T_p \geq T_{dp} - \Delta_s \\ 1 & T_p < T_{dp} - \Delta_s \end{cases} \tag{2}$$

where T_p is the water temperature of the pool; T_{dp} is the design water temperature of the pool; Δ_s is a threshold set by the user to ensure the thermal comfort of the pool.

LC is the entire cost including the initial investment and operating cost incurred within the project lifetime, which is expressed as the following equation:

$$LC = ic + oc \tag{3}$$

where ic and oc are the initial and operation costs, respectively. The ic comprises the initial cost of the PST, ASHPs, and other components, which is expressed as the following equation:

$$ic = ic_p + ic_a + ic_o \tag{4}$$

where ic_p, ic_a, and ic_o are the initial costs of the PST, ASHPs, and other components, respectively.

The oc incurred within the lifetime of the project is expressed as the following equation [5]:

$$oc = oc_1 \sum_{i=1}^{k} ((1+r)/(1+a))^{k-1} \tag{5}$$

where oc_1 is the operating cost in the first year within the lifetime of the project; r is the rate of electricity increase; a is the discount rate in the market.

Both single-objective and double-objectives optimizations were considered in the TEO process. In the single-objective optimization, the TP was set as 0%; hence, minimizing the LC is the only optimization objective. In the double-objective optimization, a Pareto optimal solution (POS) set was applied to demonstrate the optimal combination of the TP and LC. Compared with the only solution in the optimization process, the POS set is more meaningful when addressing practical problems [17].

2.3. Range of design variables

The ranges of the V_{pst} and q_{ashp} were identified according to the minimum and maximum thermal requirements of the heating system in different operating periods. Fig. 2 shows the method for identifying the maximum size of the main components. The required maximum thermal energy during the open period (te_o) and that during the preheating period (te_p) were calculated using the heat transfer models of the pool without and with a thermal-insulation cover, respectively. In addition, the worst-case scenario will be used to identify the weather conditions.

The maximum design value of the V_{pst} (V_{pm}) was identified for satisfying the maximum thermal energy requirement during the open period, which is expressed as the following equation:

$$V_{pm} = \frac{te_o}{(1-\varepsilon_w)\rho_{pm}[c_s(T_m - T_{dp}) + c_l(T_{dt} - T_m)] + \varepsilon_w c_w \rho_w (T_{dt} - T_{dp}) + (1-\varepsilon_w)\rho_{pm}\Delta H_m} \tag{6}$$

where ε_w denotes the water fraction; ρ_{pm} denotes the PCM density; c_s and c_l denote the solid and liquid PCM specific heat, respectively; T_m denotes the melting temperature of the PCM; T_{dt} denotes the design temperature that the PST should be heated to during the charging process; c_w and ρ_w denote the water specific heat and density, respectively; ΔH_m denotes the latent heat of the PCM.

The maximum design value of the q_{ashp} (q_{am}) was identified for satisfying two aims, i.e., realizing the charging process of the PST and the thermal energy requirement during the preheating period. For the first aim, the relevant equation is expressed as follows:

$$q_{amc} = \frac{te_o}{\Delta t_c} \tag{7}$$

where q_{amc} denotes the required heating capacity of the ASHPs for charging; Δt_c denotes the time span of the charging process. For the second aim, the relevant equation is expressed as follows:

$$q_{amp} = \frac{te_p}{\Delta t_p} \tag{8}$$

where q_{amp} denotes the required heating capacity of the ASHPs for preheating; Δt_p denotes the time span of the preheating process. Here, q_{am} should be equal to the maximum value between q_{amc} and q_{amp}.

The minimum design values of V_{pst} (V_{pn}) and q_{ashp} (q_{an}) were identified considering the practical minimum of the system configuration, which was assessed using a user-defined factor φ_n. Hence, V_{pn} and q_{an} are expressed as the following equations:

$$V_{pn} = \varphi_n V_{pm} \tag{9}$$

$$q_{an} = \varphi_n q_{am} \tag{10}$$

2.4. Response Surface Approach

To enhance the calculation efficiency during the optimization process, it is important to develop surrogate models rather than using the complex simulation platform [18-20]. The RSA is considered as a prominent tool for constructing surrogate models and is mathematically formulated as follows [21, 22]:

$$W = a_0 + \sum_{k=1}^{v} a_k Y_k + \sum_{k=1}^{v} a_{kk} Y_k^2 + \sum_{k<j}^{v} a_{kj} Y_k Y_j + ee \tag{11}$$

where W denotes the response parameter; a_0 denotes the intercept value; a_k denotes the first-order factor; a_{kk} denotes the second-order factor; a_{kj} denotes the interaction effect coefficient; ee denotes the random error; Y_k and Y_j denote the decision variables.

2.5. Non-dominated Sorting Genetic Algorithm II

NSGA-II is an advanced version of the NSGA, which has been proven effective in obtaining better solutions and convergence than other optimal algorithms [23, 24]. Fig. 3 shows the basic flowchart of the NSGA-II, which includes imitating the natural evolution procedure (i.e., selection, crossover, and mutation), non-dominated and elitism sorting mechanism.

2.6. Performance indices

To analyze the performance of the heating system with the optimal combinations of V_{pst} and q_{ashp}, three performance indices were used, shown as follows.

(a) Energy saving ratio (e_{sr})

The energy saving ratio (e_{sr}) is defined as the energy use difference between the developed and traditional heating systems (e.g., electrical heaters), divided by the energy use of the traditional heating system. It is expressed as the following equation:

$$e_{sr} = \frac{e_t - e_d}{e_t} \times 100\% \tag{12}$$

where e_t and e_d denote the energy use of the traditional and developed heating systems, respectively.

(b) Operating cost saving ratio (oc_{sr})

The operating cost saving ratio (oc_{sr}) is defined as the operating cost difference between the adopted and traditional heating systems, divided by the operating cost of the traditional heating system. It is expressed as the following equation:

$$oc_{sr} = \frac{oc_{ts} - oc_{ds}}{oc_{ts}} \times 100\% \tag{13}$$

where oc_{ts} and oc_{ds} denote the operating cost of the traditional and developed heating systems, respectively.

(c) Simple payback period (sp_p)

The simple payback period (sp_p) is defined as the initial investment of the developed heating system, divided by the operating cost difference between the developed and traditional heating systems. It is expressed as the following equation:

$$sp_p = \frac{ic_{ds}}{oc_{ts} - oc_{ds}} \tag{14}$$

where ic_{ds} denote the initial investment of the developed heating system.

3. Open-air swimming pool heating system and simulation platform

3.1. Open-air swimming pool heating system

The schematic of the proposed heating systems is shown in Fig. 4, which includes a PST, ASHPs, thermal-insulation cover, heat exchangers, valves, and pumps. The PST is adopted to store the heat provided by the ASHPs during the off-peak period and release it to the pool during the on-peak period. Hence, the electricity consumed is shifted from the on-peak to off-peak periods, which efficiently reduces the operating cost. The ASHPs were adopted to not only charge the PST, but also preheat the pool. The cover was used to reduce heat losses from the pool during the close period.

3.2. Control strategies

Two major control strategies were used for operating the system: time-based and temperature-based controls.

3.2.1 Time-based control

Table 1 presents the rated operating actions of the main components in a 24-h operation period. From δ_0 to δ_3 and from δ_4 to δ_0, the cover was placed on the surface of the pool; from δ_3 to δ_4, it was removed from the surface of the pool. From δ_0 to δ_1, the PST was utilized to store the heat collected from the ASHPs; from δ_3 to δ_4, it released heat into the pool. From δ_0 to δ_1, the ASHPs were utilized to charge the PST; from δ_1 to δ_2, they were utilized to preheat the pool water. From δ_4 to δ_5 and from δ_2 to δ_4, the on-peak electricity was used; from δ_5 to δ_2, the off-peak electricity was used.

3.2.2 Temperature-based control

The aim of the temperature-based control is to realize the rated water temperature profile of the heating system, as shown in Fig. 5. Three basic control strategies were developed in the temperature-based control: PST charging, preheating, and heating controls.

(a) PST charging control

The on/off controller was utilized for this control. ASHPs and associated pumps were opened to store heat into the PST at δ_0; they were closed when the temperature of the PST reached the set temperature value T_{dt}.

(b) Preheating control

The on/off controller was utilized for this control. ASHPs and associated pumps were opened to preheat the pool water at δ_1; they were closed when the water temperature of the pool reached the set temperature value $T_{dp} + \Delta_l$.

(c) Heating control

A PI controller was utilized for this control. The PI controller measured the water temperature value of the pool constantly and compared it with the set design temperature value T_{dp}. According to the error between the measured and set values, the water flowrate of the pumps for discharging the PST was adjusted to maintain the water temperature of the pool at T_{dp}.

3.3. Simulation platform

TRNSYS and MATLAB were utilized to construct the simulation platform of the system. The operation of the system was modeled in the TRNSYS 17 environment. ASHPs with the rated COP of 5.5 were simulated using Type 941. Pumps were modeled by Type 3b. Type 91 was adopted to simulate the heat exchanger with the effectiveness of 0.95. Mixing valves and diverting valves were modeled using Type 649 and Type 647, respectively. Type 23 was used as the PID controller to implement the water temperature control of the pool during the open period. MATLAB was used to program the heat transfer models of the PST and pool. Type 155 that was the interface between TRNSYS and MATLAB was utilized to integrate these models into TRNSYS.

3.3.1 Open-air swimming pool model

The water temperature variation of the pool was affected by the total heat that flows in and out of the pool; hence, it is expressed by the following equation [25, 26]:

$$\rho_w c_w V_p \frac{dT_p}{dt} = q_t \tag{15}$$

where T_p and V_p denote the water temperature and volume of the pool, respectively; q_t denotes the total heat transfer rate of the pool. During the open period when the cover is removed from the surface of the pool, q_t comprises heat obtained from solar [5], heat obtained from the PST, evaporative heat loss [27], convective heat loss [5], radiative heat loss [28], conductive heat loss [29], and heat loss resulted from refilling fresh water [25]. During the close period when the cover is placed in the surface of the pool, q_t comprises heat obtained from the ASHPs, conductive heat loss [29], and heat loss from the cover.

The heat resulting from the PST or ASHPs (q_{pa}) is expressed as following equation:

$$q_{pa} = c_w m_w (T_{pao} - T_{pai}) \tag{16}$$

where m_w denotes the water flowrate; T_{pai} and T_{pao} denote the inlet and outlet water temperatures of the heat exchanger in the load side, respectively.

The heat loss from the cover (q_{lt}) is expressed as the following equation:

$$q_{lt} = h_{tp} A_t (T_p - T_c) \tag{17}$$

where h_{tp} denotes the heat transfer coefficient between the cover and pool; A_t denotes the area of the cover; T_c denotes the temperature of the cover.

3.3.2 PCM storage tank model

To simplify the heat transfer model of the PST, the following assumptions are proposed: (i) no heat source exists inside the PCM tubes; (ii) the effect of temperature variations on the thermal parameters of both the water and the PCM are ignored; (iii) the temperature of the PCM is unaltered when during the phase change transition; (iv) variations in temperature along the directions except the water flow direction are ignored; (v) no heat exchange occurs between the PST and the ambient environment. Fig. 6 depicts the schematic of the heat transmission in the PST.

Based on the aforementioned assumptions, the governing equations for the heat transmission process between the water and the PCM are presented as follows. For the water side, the following equation holds:

$$\rho_w c_w \varepsilon_w \frac{\partial T_w}{\partial t} + \rho_w c_w \varepsilon_w v_w \frac{\partial T_w}{\partial x} = k_w \varepsilon_w \frac{\partial^2 T_w}{\partial^2 x} + h_t \left(T_{pm} - T_w\right) \tag{18}$$

where T_w, v_w, and k_w denote the temperature, mean velocity, and thermal conductivity of water, respectively; T_{pm} denotes the temperature of the PCM; h_t denotes the volumetric heat transfer coefficient between the water and the PCM; t and x denote the time and distance, respectively.

For the PCM side, the following equation holds:

$$\rho_{pm}(1-\varepsilon_w)\frac{\partial H_{pm}}{\partial t} = h_t\left(T_w - T_{pm}\right) \tag{19}$$

where H_{pm} denotes the enthalpy of the PCM, which is depicted as the following equation:

$$H_{pm} = c_{pm}T_{pm} + f_{pm}\Delta H_m \tag{20}$$

where f_{pm} denotes the melting or solidification fraction of the PCM, which is depicted as the following equation:

$$\begin{cases} f_{pm} = 0 & T_{pm} < T_m \\ 0 < f_{pm} < 1 & T_{pm} = T_m \\ f_{pm} = 1 & T_{pm} > T_m \end{cases} \tag{21}$$

The finite difference method is utilized to discretize the governing energy balance equations, i.e., Eqns. (18) and (19) [31, 32]. The discretized algebraic equations are shown as follows:

$$\rho_w c_w \varepsilon_w\left(\frac{T_{w,i}^{j+1} - T_{w,i}^{j}}{\Delta t} + v_w\frac{T_{w,i}^{j+1} - T_{w,i-1}^{j+1}}{\Delta x}\right) = k_w\varepsilon_w\frac{T_{w,i+1}^{j+1} - 2T_{w,i}^{j+1} + T_{w,i-1}^{j+1}}{\Delta x^2} + h_t\left(T_{pm,i}^{j+1} - T_{w,i}^{j+1}\right) \tag{22}$$

$$\rho_{pm}(1-\varepsilon_w)\frac{H_{pm,i}^{j+1} - H_{pm,i}^{j}}{\Delta t} = h_t\left(T_{w,i}^{j+1} - T_{pm,i}^{j+1}\right) \tag{23}$$

As shown in Fig. 6, the volume in each row along the water flow direction was selected as one heat transfer finite element. MATLAB programs were used to solve the discretized algebraic equations.

4. Case study

The swimming pool located at the City University of Hong Kong, where the climate is subtropical, was selected as the application object of the proposed heating system. The total volume of the pool is 1963.5 m^3. Its width and length are 22 and 50 m, respectively. Its minimum depth is 1.2 m, which appears on both sides of the pool; its maximum depth is 2.5 m, which appears in the middle of the pool. The pool cannot be used for swimming from December to next April because the water temperature is low, especially when heating measures are not implemented. Therefore, the pool is closed, which results in the waste of the facility and space.

The proposed heating system was applied for this pool to extend the available time during the winter. The important times of this system in a 24-h operation schedule are proposed as follows. The moment for starting the charge of the PST is at 21:00 (δ_0); the moment for preheating the pool water is at 05:00 (δ_1); the moments for opening and closing the swimming pool facility are at 12:00 (δ_3) and 20:00 (δ_4), respectively; the moments for using the on-peak and off-peak electricity are at 09:00 (δ_2) and 21:00 (δ_5), respectively. Sodium acetate trihydrate, which has a large latent heat, was selected as the PCM, and its thermal properties are listed in Table 2. Table 3 summarizes the unit costs of the main components in the heating system.

5. Results and analysis

5.1. Development and validation of surrogate models

To develop surrogate models of different objective functions, the central composite design (CCD) method was adopted to generate the design of experiments (DOE) scheme, which was realized using the DESIGN EXPERTS software. The maximum thermal energy requirement of the pool during the open period that was identified at the design day (occurring on February 26th, 2005) was 5.2×10^7 kJ. The factor for determining the minimum size of the system configuration (φ_n) was set to 10%. Hence, the range for the PST volume (V_{pst}) was from 13.6 ^{3} to 135.8 m^3, and the range for the heating capacity of the ASHPs (q_{ashp}) was from 60.2 to 601.7 kW.

Table 4 shows the CCD-based DOE scheme and the corresponding simulated results. The simulated values of TP and LC were acquired by inputting the values of V_{pst} and q_{ashp} into the constructed simulation platform of system, respectively. It should be noted that the design values of V_{pst} and q_{ashp} in Cases 2, 3, 5, 10, and 11 were the same because they were central points in the CCD plan. Five replications of central points can enable a reasonable evaluation of random errors [34]. To calculate the operating cost in Eqn. (5), the rate for the electricity increase (r) and the discount rate in the market (a) were set as 4.3% and 7.3%, respectively [5]. In addition, ten-winter (from 2003 to 2013) meteorological data in Hong Kong that were collected from the Hong Kong Observatory were input into the simulation platform, and the average annual operating cost was considered as the operating cost in the first year within the lifetime of the project (oc_1) in Eqn. (5). The length of the project was assumed to be 10 years. It was observed in Case 9 that when both the V_{pst} and q_{ashp} were the maximum, the TP and LC were 0% and HK$6,017,343, respectively; in Case 4, when both the V_{pst} and q_{ashp} were the minimum, the TP and LC were 7.73% and HK$1,197,438, respectively. This suggested that although the LC was reduced by 80.1% when the size of the system varied from the maximum to the minimum, the thermal comfort unmet time was increased by 7.73%.

Fig. 7 shows the comparisons between the predicted results using surrogate models and the simulated results from the simulation platform. The surrogate models developed using the RMA are expressed by the following equations:

- Linear models:

$$TP = (72214.97 - 92.48V_{pst} - 135.72q_{ashp}) \times 10^{-6} \tag{24}$$

$$LC = 614169 + 4606.89V_{pst} + 8066.62q_{ashp} \tag{25}$$

- Quadratic models:

$$TP = (111144 - 327.08V_{pst} - 432.98q_{ashp} - 0.15V_{pst}q_{ashp} + 1.90V_{pst}^2 + 0.47q_{ashp}^2) \times 10^{-6} \tag{26}$$

$$LC = 502385 + 7173.75V_{pst} + 8996.35q_{ashp} + 7.96V_{pst}q_{ashp} + 34.82V_{pst}^2 - 2.30q_{ashp}^2 \tag{27}$$

As shown, the predicted R^2 of the linear models for the objective functions of TP and LC were 0.5656 and 0.9881, respectively; the predicted R^2 of the quadratic models for the objective functions of TP and LC were 0.9791 and 0.9987, respectively. Regardless of the TP or LC, the predicted R^2 values using the quadratic models were higher than those using the linear models, which indicated that the quadratic models were more reliable and suitable as surrogate models.

5.2. Single-objective optimization

The TP was predefined as 0% during the optimization process, which was regarded as the design constraint in the single-objective optimization. Minimizing the LC was the only optimization objective. Fig. 8 shows the single-optimization process using the GA, which demonstrates the variation in LC with the generations; 1500 generations were performed during the optimization. The optimal LC was identified in approximately 800 generations and was maintained for approximately 700 generations (from 800 generations to 1500 generations). After the single-objective optimization was performed, the lowest LC was acquired, i.e., HK$3,846,263. Accordingly, the optimal volume of the PST (V_{pst}) and the heating capacity of the ASHP (q_{ashp}) were 80.0 m^3 and 338.0 kW, respectively.

5.3. Double-objectives optimization

Minimizing both the LC and TP were the objectives of the double-objective optimization. Fig. 9 shows the POS sets during the double-objective optimization process that was performed using NSGA-II. Unlike the single-objective optimization where only one solution is optimal, all combinations of LC and TP are optimal solutions for the system design in the double-objective optimization. If the solution with a lower TP is selected as the optimal solution, then LC will be higher than the LC in other solutions; conversely, if the solution with a lower LC is selected as the optimal solution, then TP will be higher than the TP in other solutions. The optimal LC when TP was selected as 0% in the double-objective optimization was HK$3,845,937, which was slightly lower than that in the single-objective optimization. The reason might be that the NSGA-II adopted in the double-objective optimization was more advanced than the GA adopted in the single-objective optimization. The LC of the system can be reduced when the TP is increased. The LC of the system was HK$1,190,654 when the TP was selected as 8%, which was 69.04% less than that when the TP was selected as 0%.

Table 5 summarizes the TEO results for different desired TPs. The values of V_{pst} and q_{ashp} can be reduced when the TP increases, which means that the required sizes of the main components can be decreased by sacrificing the thermal comfort of the pool. The V_{pst} and q_{ashp} were 80.6 m^3 and 337.6 kW when the desired TP was 0%, respectively; the V_{pst} and q_{ashp} were 13.7 m^3 and 66.6 kW when the desired TP was 8%, respectively. Hence, the V_{pst} and q_{ashp} were reduced by 83.0% and 80.3% when the desired TP varied from 0% and 8%, respectively.

5.4 Performance analysis after optimization

In this section, the desired TP is set as 0% to analyze the system performance after optimization. The corresponding optimal volume of the PST (V_{pst}) and the heating capacity of the ASHPs (q_{ashp}) are 80.6 m^3 and 337.6 kW, respectively. The control, energy, and economic performance analysis of the system with the optimal configuration are presented as follows.

(a) Control performance analysis

Fig. 10 shows the water temperature variations of the pool within a week (from January 17, 2010 to January 23, 2010). The water temperature of the pool (T_p) increased during the preheating period. After the preheating period, the T_p reduced until the open period as no heat was supplied into the pool. Because the PI controller was utilized, the T_p during the open period was well maintained at approximately 28 °C, indicating that the thermal comfort of the pool could be satisfied.

(b) Energy performance analysis

Fig. 11 depicts the energy saving ratio (e_{sr}) of the heating system with the optimal design configuration in different winter seasons (from 2003 to 2012). The maximum e_{sr} and minimum e_{sr} are 73.7% and 72.1%, respectively, which occurred in 2006 and 2010, respectively; and the average e_{sr} is 72.8%. The average energy use of the developed heating system (e_d) with the optimal configuration is 1.07 × 10^9 kJ. Compared with the developed heating system with the maximum sizing configuration (Case 9) with e_d of 1.57 × 10^9 kJ, the e_d is reduced by 31.8%.

(c) Economic performance analysis

Fig. 12 shows the operating cost saving ratio (oc_{sr}) of the heating system with optimal design configuration in different winter seasons (from 2003 to 2012). The maximum oc_{sr} and minimum oc_{sr} are 82.6% and 79.0%, respectively, which occurred in 2005 and 2006, respectively; and the average oc_{sr} is 81.1%. The average operating cost of the developed heating system (oc_{ds}) with optimal configuration is HK$252,242. Compared with the adopted heating system with the maximum sizing configuration (Case 9) that has the oc_{ds} of HK$370,668, the oc_{ds} is reduced by 32.0%. The initial cost of the system (ic_{ds}) with the optimal design configuration is HK$1,606,871. Compared with Case 9 with the ic_{ds} of HK$2,743,893, the ic_{ds} is reduced by 41.4%. The simple payback period of the system with the optimal design configuration is 1.48 years, which indicates that the ic_{ds} can be rapidly recovered.

6. Conclusions

A TEO approach for a heating system was proposed in this study to minimize the lifecycle cost of the system while ensuring the desired thermal comfort. The design variables were the PST volume and the heating capacity of ASHPs. A case study of a typical swimming pool in Hong Kong that used the proposed heating system to extend the time available to use it in winter was presented to illustrate the proposed optimization approach. The DESIGN EXPERTS software was utilized for generating a dataset of design variables based on predefined ranges of design variables. Subsequently, the generated dataset of design variables was input to the simulation platform of the system that was established by combining MATLAB and TRNSYS. The corresponding values of the objective functions including the TP and LC were obtained. Based on the DOE scheme, the RSA was used for developing surrogate models for the objective functions. Single-objective and double-objective optimizations were conducted using the GA and NAGA-II, respectively. The optimal solutions for sizing the main components were ascertained. The results of system performance for the optimal system configuration indicated that the average energy saving ratio and economic saving ratio were 72.8% and 81.1%, respectively, when compared with the traditional heating system. Furthermore, the energy and economic performance of the system with the optimal system configuration were significantly higher than those with the maximum size of main components. Hence, the proposed TEO method is highly instructive and important for optimally sizing swimming pool heating systems.

Acknowledgement

The authors sincerely thank the anonymous reviewers for their time and effort. In addition, the authors appreciate the support of Dr. Gongsheng Huang.

References

[1] A. Mousia, A. Dimoudi, Energy performance of open air swimming pools in Greece, Energy and Buildings 90 (2015) 166-172.

[2] Y. Yadav, G. Tiwari, Analytical model of solar swimming pool: transient approach, Energy conversion and management 27(1) (1987) 49-54.

[3] J. Francey, P. Golding, R. Clarke, Low-cost solar heating of community pools using pool covers, Solar Energy 25(5) (1980) 407-416.

[4] W.W. Chan, J.C. Lam, Energy-saving Supporting Tourism Sustainability: A Case Study of Hotel Swimming Pool Heat Pump, Journal of Sustainable Tourism 11(1) (2003) 74-83.

[5] J.C. Lam, W.W. Chan, Life cycle energy cost analysis of heat pump application for hotel swimming pools, Energy Conversion and Management 42(11) (2001) 1299-1306.

[6] Y. Li, G. Huang, H. Wu, T. Xu, Feasibility study of a PCM storage tank integrated heating system for outdoor swimming pools during the winter season, Applied Thermal Engineering 134 (2018) 490-500.

[7] G. Comodi, F. Carducci, J.Y. Sze, N. Balamurugan, A. Romagnoli, Storing energy for cooling demand management in tropical climates: A techno-economic comparison between different energy storage technologies, Energy 121 (2017) 676-694.

[8] F. Bruno, N.H.S. Tay, M. Belusko, Minimising energy usage for domestic cooling with off-peak PCM storage, Energy and Buildings 76 (2014) 347-353.

[9] A. Najafian, F. Haghighat, A. Moreau, Integration of PCM in domestic hot water tanks:

Optimization for shifting peak demand, Energy and Buildings 106 (2015) 59-64.

[10] D.N. Nkwetta, P.-E. Vouillamoz, F. Haghighat, M. El Mankibi, A. Moreau, K. Desai, Phase change materials in hot water tank for shifting peak power demand, Solar Energy 107 (2014) 628-635.

[11] G. Zsembinszki, M.M. Farid, L.F. Cabeza, Analysis of implementing phase change materials in open-air swimming pools, Solar Energy 86(1) (2012) 567-577.

[12] Z. Tian, S. Zhang, J. Deng, J. Fan, J. Huang, W. Kong, B. Perers, S. Furbo, Large-scale solar district heating plants in Danish smart thermal grid: Developments and recent trends, Energy conversion and management 189 (2019) 67-80.

[13] Z. Tian, B. Perers, S. Furbo, J. Fan, Thermo-economic optimization of a hybrid solar district heating plant with flat plate collectors and parabolic trough collectors in series, Energy conversion and management 165 (2018) 92-101.

[14] A. Kaabeche, R. Ibtiouen, Techno-economic optimization of hybrid photovoltaic/wind/diesel/battery generation in a stand-alone power system, Solar Energy 103 (2014) 171-182.

[15] M.H. Amrollahi, S.M.T. Bathaee, Techno-economic optimization of hybrid photovoltaic/wind generation together with energy storage system in a stand-alone micro-grid subjected to demand response, Applied Energy 202 (2017) 66-77.

[16] M. Jamshidi, A. Askarzadeh, Techno-economic analysis and size optimization of an off-grid hybrid photovoltaic, fuel cell and diesel generator system, Sustainable Cities and Society 44 (2019) 310-320.

[17] T. Ma, H. Yang, L. Lu, J. Peng, Pumped storage-based standalone photovoltaic power generation system: Modeling and techno-economic optimization, Applied Energy 137 (2015) 649-659.

[18] A. Sharma, N.A. Ansari, A. Pal, Y. Singh, S. Lalhriatpuia, Effect of biogas on the performance and emissions of diesel engine fuelled with biodiesel-ethanol blends through response surface methodology approach, Renewable Energy 141 (2019) 657-668.

[19] V. Yaliwal, N. Banapurmath, V. Gaitonde, M. Malipatil, Simultaneous optimization of multiple operating engine parameters of a biodiesel-producer gas operated compression ignition (CI) engine coupled with hydrogen using response surface methodology, Renewable

energy 139 (2019) 944-959.
[20] Y. Du, B. Blocken, S. Pirker, A novel approach to simulate pollutant dispersion in the built environment: transport-based recurrence CFD, Building and Environment (2019) 106604.
[21] Y. Du, C.M. Mak, Y. Li, Application of a multi-variable optimization method to determine lift-up design for optimum wind comfort, Building and Environment 131 (2018) 242-254.
[22] Y. Du, C.M. Mak, Y. Li, A multi-stage optimization of pedestrian level wind environment and thermal comfort with lift-up design in ideal urban canyons, Sustainable Cities and Society 46 (2019).
[23] Y. Xie, P. Hu, N. Zhu, F. Lei, L. Xing, X. Linghong, Collaborative optimization of ground source heat pump-radiant ceiling air conditioning system based on response surface method and NSGA-II, Renewable Energy (2019).
[24] X. Gao, Y. Tian, B. Sun, Multi-objective optimization design of bidirectional flow passage components using RSM and NSGA II: A case study of inlet/outlet diffusion segment in pumped storage power station, Renewable energy 115 (2018) 999-1013.
[25] A. Buonomano, G. De Luca, R.D. Figaj, L. Vanoli, Dynamic simulation and thermo-economic analysis of a PhotoVoltaic/Thermal collector heating system for an indoor–outdoor swimming pool, Energy Conversion and Management 99 (2015) 176-192.
[26] A. Somwanshi, A.K. Tiwari, M.S. Sodha, Feasibility of earth heat storage for all weather conditioning of open swimming pool water, Energy Conversion and Management 68 (2013) 89-95.
[27] C. Smith, R. Jones, G. Lof, Energy requirements and potential savings for heated indoor swimming pools, ASHRAE Transactions-American Society of Heating Refrigerating Airconditioning Engin 99(2) (1993) 864-876.
[28] E. Ruiz, P.J. Martínez, Analysis of an open-air swimming pool solar heating system by using an experimentally validated TRNSYS model, Solar Energy 84(1) (2010) 116-123.
[29] T.L. Bergman, F.P. Incropera, Fundamentals of heat and mass transfer, John Wiley & Sons2011.
[30] Y. Li, G. Huang, T. Xu, X. Liu, H. Wu, Optimal design of PCM thermal storage tank and

its application for winter available open-air swimming pool, Applied Energy 209 (2018) 224-235.
[31] S. Wu, G. Fang, Dynamic performances of solar heat storage system with packed bed using myristic acid as phase change material, Energy and Buildings 43(5) (2011) 1091-1096.
[32] H. Peng, R. Li, X. Ling, H. Dong, Modeling on heat storage performance of compressed air in a packed bed system, Applied Energy 160 (2015) 1-9.
[33] J. Pereira da Cunha, P. Eames, Thermal energy storage for low and medium temperature applications using phase change materials – A review, Applied Energy 177 (2016) 227-238.
[34] M.B. Salehi, M.V. Sefti, A.M. Moghadam, A.D. Koohi, Study of salinity and pH effects on gelation time of a polymer gel using central composite design method, Journal of Macromolecular Science, Part B 51(3) (2012) 438-451.

Tables

Table 1 Rated operating actions of main components in a 24-h operation period

	$\delta_0 \rightarrow \delta_1$	$\delta_1 \rightarrow \delta_2$	$\delta_2 \rightarrow \delta_3$	$\delta_3 \rightarrow \delta_4$	$\delta_4 \rightarrow \delta_5$	$\delta_5 \rightarrow \delta_0$(next)
Thermal-insulation cover	cover pool surface			remove from pool surface	cover pool surface	
PST	charge	idle		discharge	idle	
ASHPs	on	on	off			

Table 2 Thermo-physical properties of used PCM [33]

Parameters	Value
Phase change temperature (℃)	58
Latent heat (kJ/kg)	266
Density (kg/m^3)	1450
Solid specific heat (kJ/kg · K)	1.68
Liquid specific heat (kJ/kg · K)	2.37
Solid thermal conductivity (W/m · K)	0.43
Liquid thermal conductivity (W/m · K)	0.34

Table 3 Unit costs of main components in the heating system

Items	Unit	Cost (HK$)
PST	m^3	2,427
ASHP	kW	1,266
Thermal-insulation cover	m^2	32
Heat exchanger	-	6,000
Pump	-	5,100
Controller	-	25,625

Table 4 CCD-based design dataset and simulation results

Case	V_{pst}(m^3)	q_{ashp}(kW)	TP(%)	LC(HK$)
1	13.6	601.7	1.041	5,227,914
2	74.7	331.0	0.018	3,772,777
3	74.7	331.0	0.018	3,772,777
4	13.6	60.2	7.735	1,197,438
5	74.7	331.0	0.018	3,772,777
6	135.8	60.2	7.667	1,459,856
7	135.8	331.0	0	3,937,180
8	13.6	331.0	2.281	3,300,143
9	135.8	601.7	0	6,017,343
10	74.7	331.0	0.018	3,772,777
11	74.7	331.0	0.018	3,772,777
12	74.7	601.7	0.003	5,837,942
13	74.7	60.2	7.690	1,321,675

Table 5 TEO results in different desired TPs

Desired TP(%)	V_{pst}(m^3)	q_{ashp}(kW)	Actual TP(%)	LC(HK$)
0	80.6	337.6	0	3,845,937
1	79.5	274.7	1.01	3,324,414
2	59.4	236.2	2.00	2,914,003
3	48.5	200.7	3.02	2,558,248
4	39.1	170.6	4.00	2,250,379
5	50.0	130.2	5.01	1,958,055
6	31.0	111.1	6.00	1,689,565
7	21.0	88.7	7.01	1,432,466
8	13.7	66.6	8.01	1,190,654

Figures

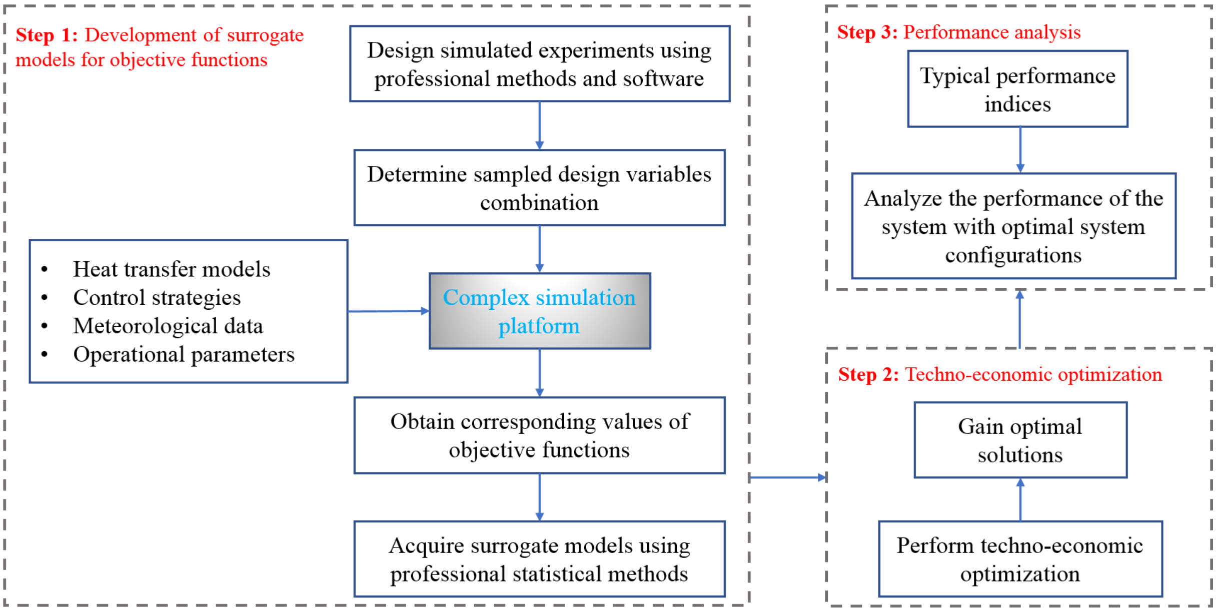

Fig. 1. Framework of TEO methodology.

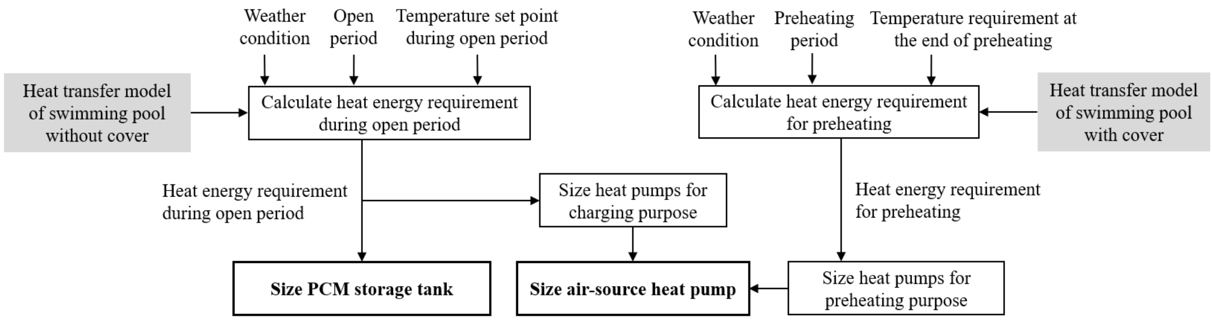

Fig. 2. Method for identifying maximum size of main components.

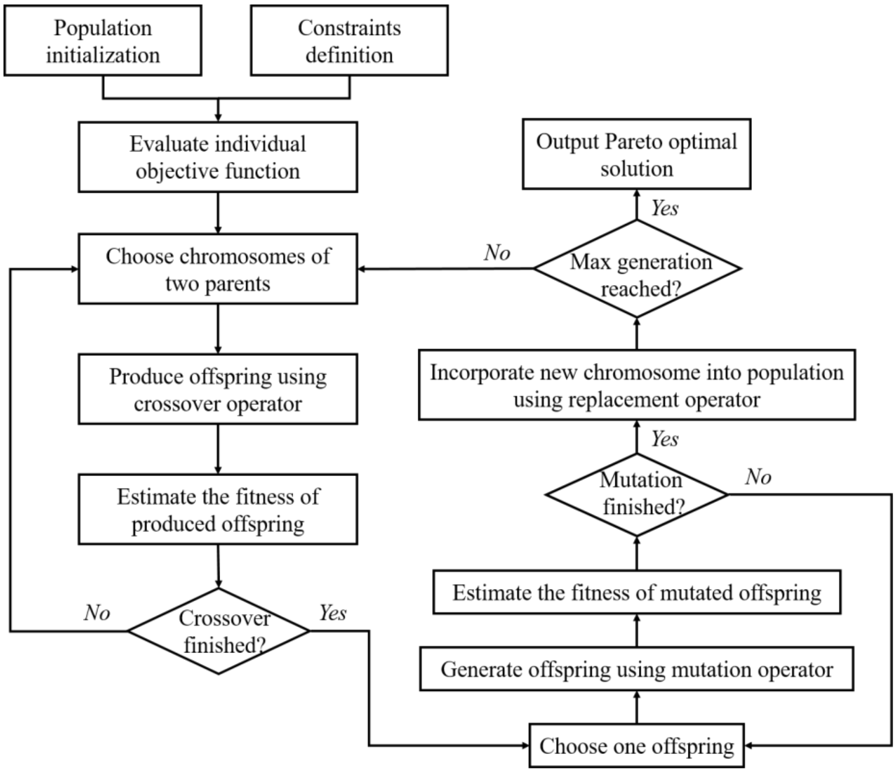

Fig. 3. Basic flowchart of NSGA-II.

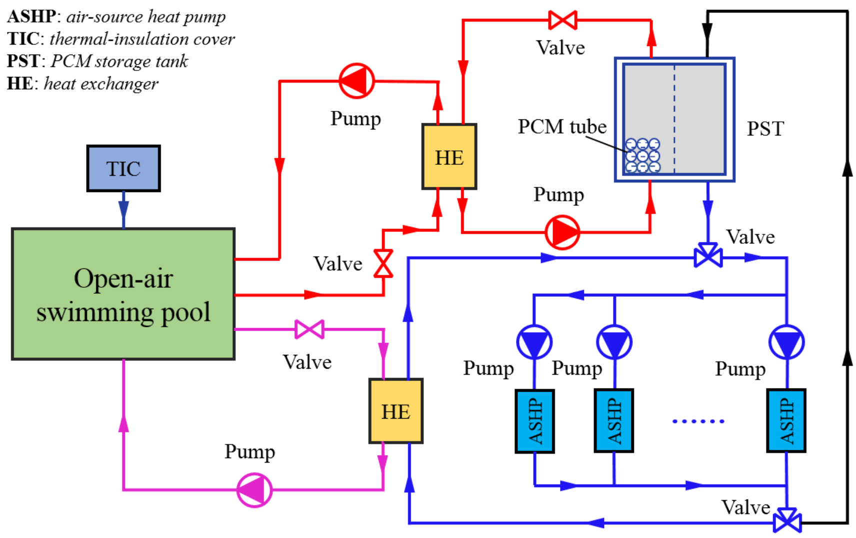

Fig. 4. Schematic of the swimming pool heating system.

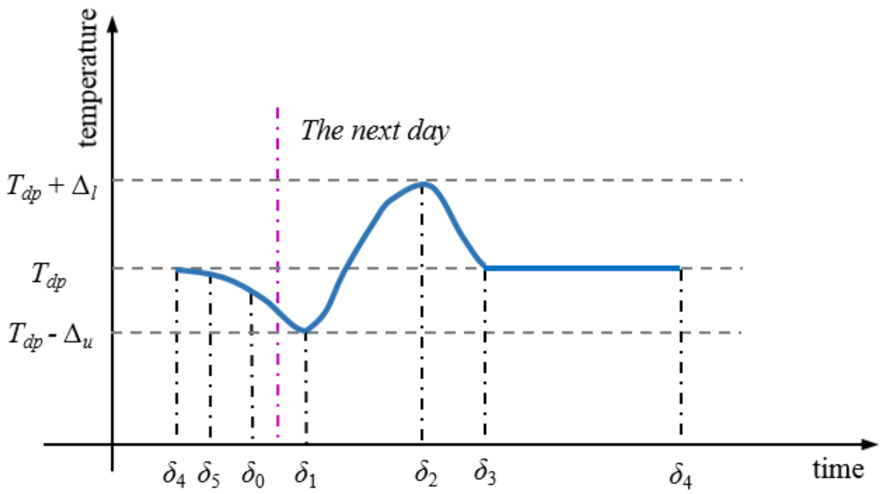

Fig. 5. Rated water temperature profile of the swimming pool heating system.

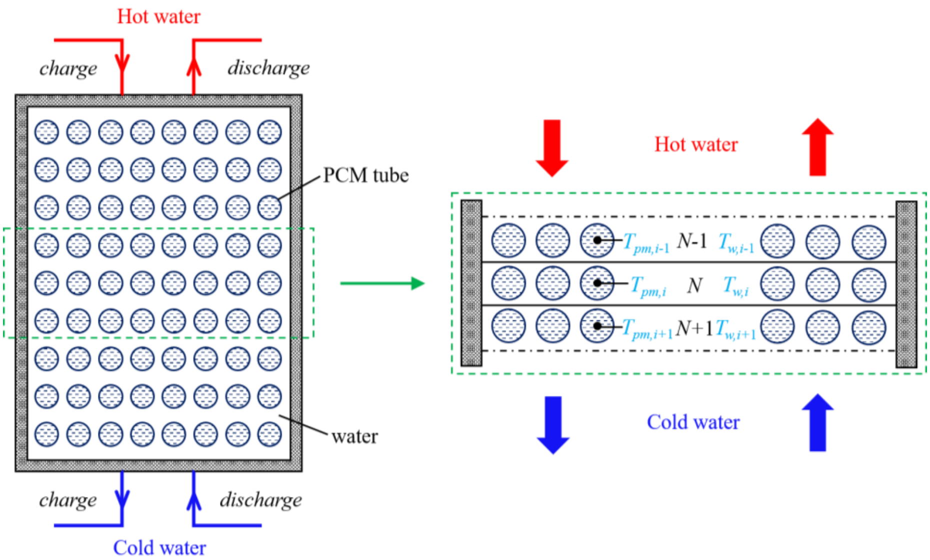

Fig. 6. Schematic of heat transmission in PST [30].

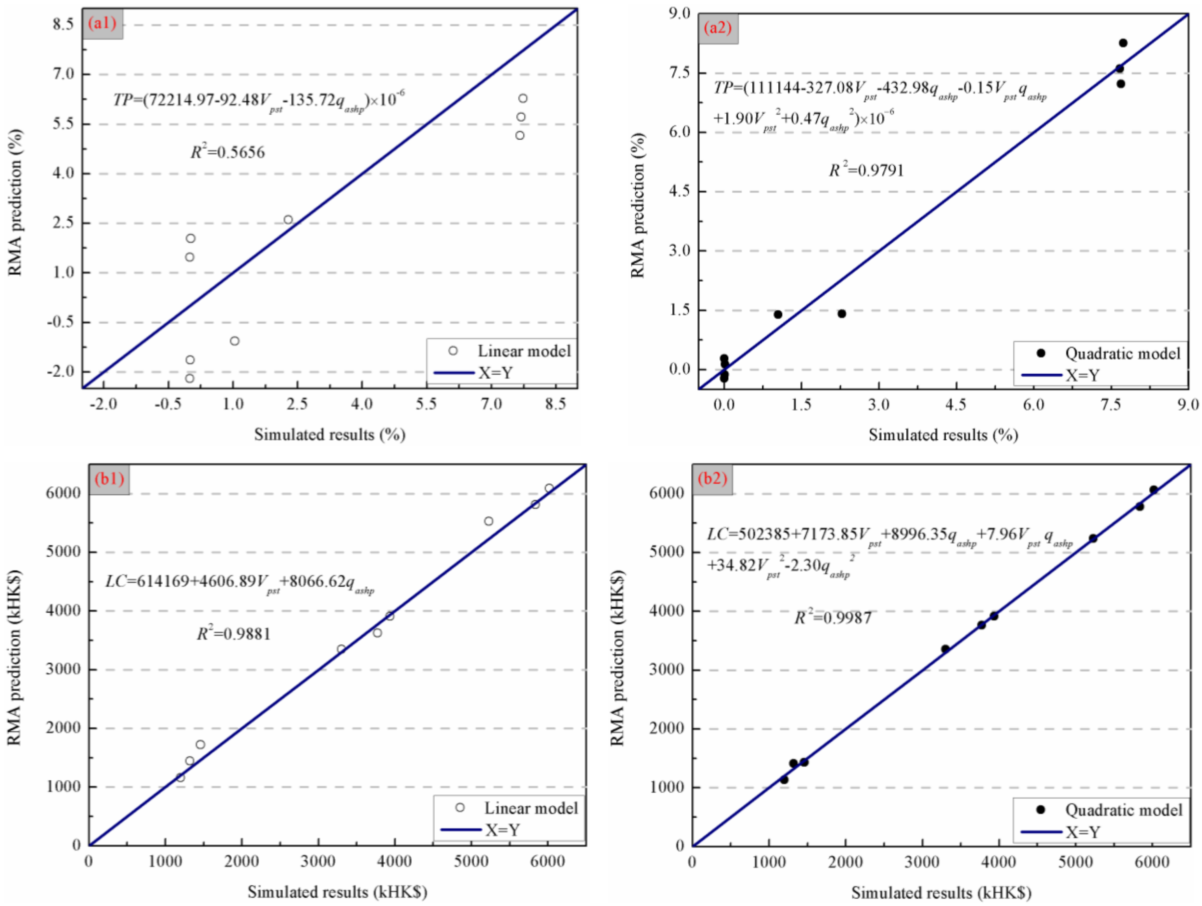

Fig. 7. Comparison between predicted results using surrogate models and simulated results from the simulation platform: (a1) Linear model of TP; (a2) Quadratic model of TP; (b1) Linear model of LC and (b2) Quadratic model of LC. (Note: "kHK$" in the graph represents HK$1,000)

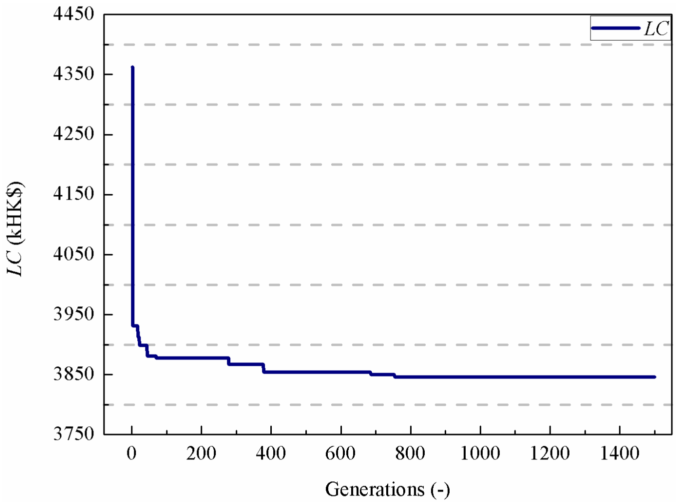

Fig. 8. Single-objective optimization process using GA.

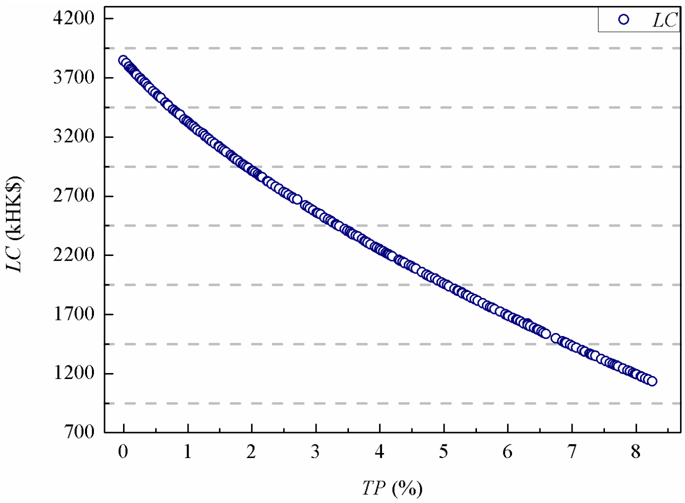

Fig. 9. POS sets during the double-optimization process.

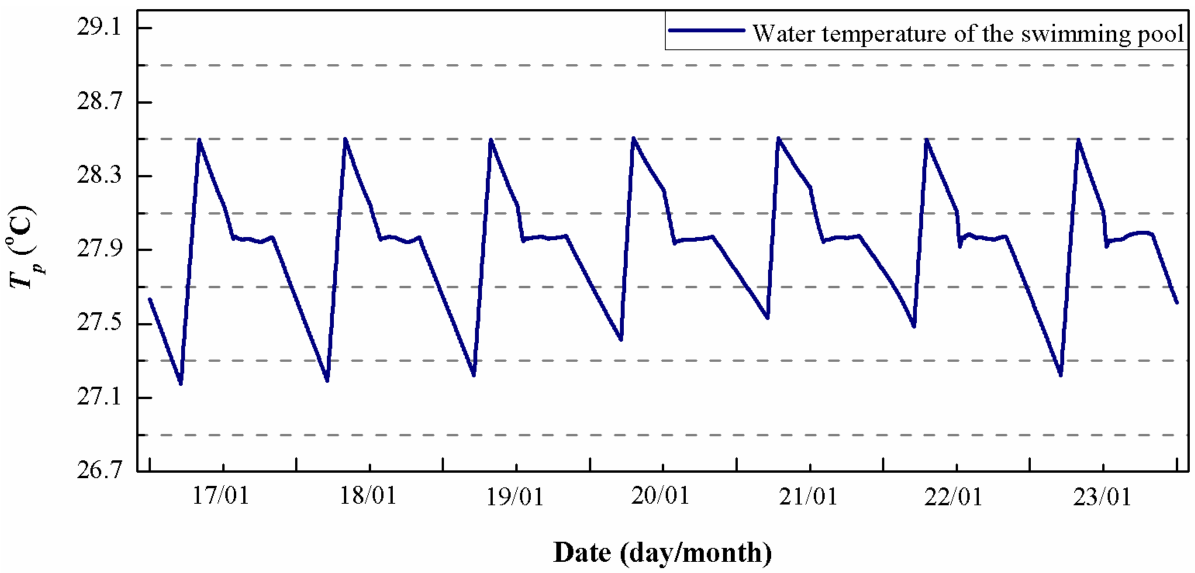

Fig. 10. Water temperature variations of the pool within a week.

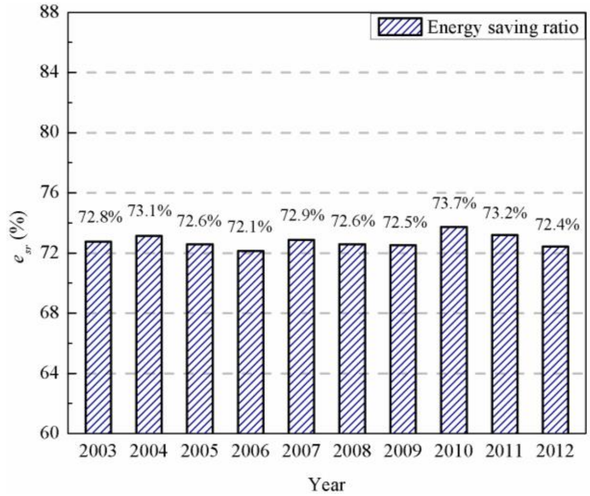

Fig. 11. e_{sr} of the system with optimal design configuration.

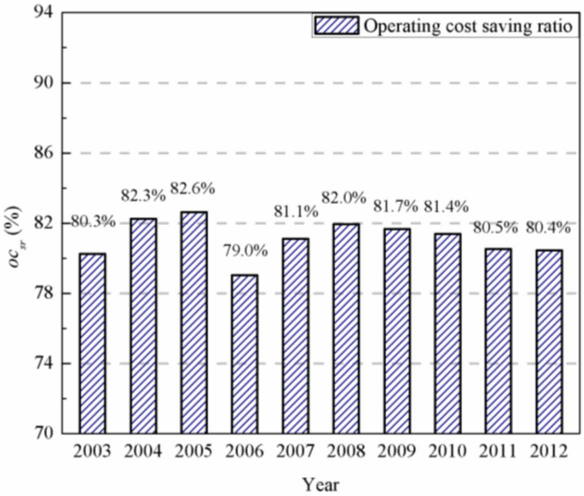

Fig. 12. oc_{sr} of the system with optimal design configuration.